energies

MDPI

Article

Properties and Simulating Research of Epoxy Resin/Micron-SiC/Nano-SiO_2 Composite

Ning Guo [1], Ruixiao Meng [1], Junguo Gao [1,*], Mingpeng He [2,*], Yue Zhang [2,*], Lizhi He [3] and Haitao Hu [1]

[1] Key Laboratory of Engineering Dielectrics and Its Application of Ministry of Education, Harbin University of Science and Technology, Harbin 150080, China; tad@hrbust.edu.cn (N.G.); mrxzyyx@163.com (R.M.); huhaitaodianqi@hrbust.edu.cn (H.H.)
[2] Dongfang Electric Machinery Co., Ltd., Deyang 618000, China
[3] Beijing Products Quality Inspection and Detection Institute, Beijing 101300, China; xssyb@bqi.org.cn
* Correspondence: gaojunguo@hrbust.edu.cn (J.G.); ligong038@126.com (M.H.); metaspark@163.com (Y.Z.)

Abstract: The dielectric behavior of insulations is a key factor affecting the development of anti-corona materials for generators. Epoxy resin (EP), as the matrix, is blended with inorganic fillers of micron SiC and nano SiO_2 to investigate the effect of micro and nano doping on the conductivity and breakdown mechanism of the composites. Using experimental and simulation analysis, it is found that the effect of nano-SiO_2 doping concentration on the conductivity is related to the dispersion of SiC particles. The lower concentration of SiO_2 could decrease the conductivity of the composites. The conductivity increases with raising the nano-SiO_2 doping concentration to a critical value. Meanwhile, the breakdown field strength of the composites decreases with the rising content of SiC in constant SiO_2 and increases with more SiO_2 when mixed with invariable SiC. When an equivalent electric field is applied to the samples, the electric field at the interface of micron particles is much stronger than the average field of the dielectric, close to the critical electric field of the tunneling effect. The density of the homopolar space charge bound to the surface of the stator bar elevates as the concentration of filled nanoparticles increases, by which a more effective Coulomb potential shield can be built to inhibit the further injection of carriers from the electrode to the interior of the anti-corona layer, thus reducing the space charge accumulation in the anti-corona layer as well as increasing the breakdown field strength of the dielectric.

Keywords: micro-nano composite materials; nonlinear conductivity; dielectric properties; composite structural model

Citation: Guo, N.; Meng, R.; Gao, J.; He, M.; Zhang, Y.; He, L.; Hu, H. Properties and Simulating Research of Epoxy Resin/Micron-SiC/Nano-SiO_2 Composite. *Energies* **2022**, *15*, 4821. https://doi.org/10.3390/en15134821

Academic Editor: Vladislav A. Sadykov

Received: 29 May 2022
Accepted: 20 June 2022
Published: 1 July 2022

1. Introduction

As an important part of the power system, the stability of the generator is affected by the stator insulation performance. The distribution of electric field at the end of the generator stator winding is not uniform and partial discharge is tended to ensue and therefore anti-corona layer component is usually added to equalize the surface electric field to improve the voltage endurance and ensure the stable operation of the generator. Consequently, developing a composite material with high breakdown strength and nonlinear conductivity is an effective way to upgrade the electric field homogenization of the anti-corona layer.

By adding inorganic nanomaterials and semiconducting fillers to polymeric insulating materials simultaneously, the breakdown strength of the composite dielectric will be productively improved, and the nonlinear conductivity will show up in the dielectric. The nonlinear properties are closely related to the filler content. Usually, when the concentration of semiconducting filler reaches a certain level or more, the composite material can reveal obvious nonlinear conductivity, and the nonlinear properties intensify as the filler concentration increases. However, the high content of semiconducting materials will lead to less breakdown strength and mechanical properties, which limits the application of

nonlinear materials [1–3]. The substances of inorganic nano-oxides can capably help the breakdown strength of materials, such as SiO_2 [4], Al_2O_3 [5], MgO [6], TiO_2 [7], ZrO_2 [8], ZnO [9], etc. The agglomeration phenomenon occurs when the nanofiller is excessively loaded due to the small size effect of nanoparticles with high surface energy, which declines the performance of nanocomposites [10–12]. The present research about nanodielectric is conducted on the interface, i.e., the nanoscale transition region between nanoparticles and polymer matrix, and the nanoparticle interface is schematically shown in Figure 1.

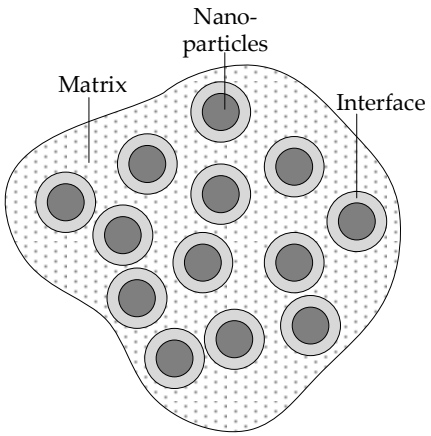

Figure 1. Schematic diagram of the nanoparticle interface.

The larger specific surface area of nanoparticles makes the interfacial region occupy a large volume fraction inside the nano-doped dielectric so that the interface will have a consequential impact on the properties of the dielectric [13]. Nonlinear anti-corona materials fixed by three substance blends in dissimilar dimensions can simultaneously regard both nonlinear conductivity and breakdown strength as important. Thereupon, it is important to probe the influence of the micron or nanofiller on the electrical properties of the composite.

In this paper, 16 specimens with different micro- and nano-doping amounts were prepared using epoxy resin (EP) cured by polyamide as the matrix, micron SiC and nano-SiO_2 as inorganic fillers via the co-blending method. The conductivity was measured by megger meter to investigate the effect of variable nano scale ingredients; the impacts of micro-and nano-doping concentrations on the breakdown field strength of the composites were discussed by AC breakdown tests; the electric field and carrier transport models at the interfaces of EP/SiC and EP/SiO_2 were established using COMSOL to investigate the distribution of internal electric field and carriers in the composites when the micro-and nano-fillers were doped.

2. Materials and Methods

2.1. Raw Materials

Bisphenol A epoxy resin E44 (EP), Nantong Xingchen Synthetic Material Co., Ltd. (Nantong, China); the curing agent is 651 low molecular polyamide resin, Beijing Xiangshan United Auxiliary Factory; micron filler is SiC, particle size 23 μm (600 mesh), its mass percentage is 20 wt%, 30 wt%, 40 wt%, 50 wt% with nano-SiO_2 modified by coupling agent γ-KH550, Beijing Deke Guiding Gold Ltd. (Beijing, China) with 1 wt%, 2 wt% by mass.

2.2. Specimen Preparation

Firstly, the appropriate amount of epoxy resin monomer was weighed and preheated to a specific temperature to reduce the viscosity. The proper amount of dried and treated nano-SiO_2 was considered according to the required mass ratio, which was combined with ultrasonic mixing for 20 min to ensure the dispersion of nanomaterials. The appropriate amount of micron SiC particles was weighed and added to the mixed melt for direct mixing. The mixing temperature is controlled to ensure that the epoxy resin is in a low viscosity

state, which facilitates the total dispersion of the micro-nano particles in the melt. The melt is integrated uniformly after sufficient stirring as well as ultrasonic dispersion time. The temperature must be controlled at 60 °C for ultrasonic degassing to remove the bubbles generated during the mechanical stirring process. The mixed melt is cooled down to room temperature and mixed with a certain measure of polyamide resin and stirred at 500 rpm until it is thoroughly mixed, after which it is again evacuated under reduced pressure to degas the mixture until no air bubbles appear in the system. The above-mentioned mixed melt after each step is poured into the mold coated with vacuum silicone grease, and the curing reaction of the melt is accelerated by the appropriate amount of heating. The curing is formed, and the micro and nanocomposite specimens are prepared for testing. The orthogonal composite filler is matched, as shown in Table 1.

Table 1. Material ratio of orthogonal composite experiment.

Specimen	Filler	Specimen	Filler
#001	1 wt% SiO_2	#002	2 wt% SiO_2
#200	20 wt% SiC	#300	30 wt% SiC
#400	40 wt% SiC	#500	50 wt% SiC
#201	20 wt%SiC + 1 wt% SiO_2	#202	20 wt% SiC + 2 wt% SiO_2
#301	30 wt% SiC + 1 wt% SiO_2	#302	30 wt% SiC + 2 wt% SiO_2
#401	40 wt% SiC + 1 wt% SiO_2	#402	40 wt% SiC + 2 wt% SiO_2
#501	50 wt% SiC + 1 wt% SiO_2	#502	50 wt% SiC + 2 wt% SiO_2

2.3. DC Conductivity Test

The DC conductivity characteristics of micron and nano SiC/SiO_2/EP composites were measured using the voltmeter–ammeter method. Two copper plate electrodes were situated in parallel onto the upper and lower surfaces of the sample disc, and a third copper concentric circle electrode connected to the earth was applied. The volumetric current was tested using a ZC36 high resistance meter with a 50 mm diameter test electrode and a 2 mm protection gap; the diameter and thickness of the test specimens were 100 mm and 500 μm, respectively. The test temperature was 20 °C.

2.4. Breakdown Field Strength Test

The effects of nano-SiO_2 doping and micron SiC doping on the AC breakdown performance of ternary composites are discussed separately. The test apparatus is a column-plate electrode with upper electrode diameter Φ1 = 20 mm and height h1 = 25 mm, lower electrode diameter Φ2 = 60 mm and height h2 = 10 mm, and the edge of the test electrode is chamfered with radius r = 2 mm to avoid the concentration of the electric field at the tip. The thickness of the test specimen is 500 μm, and the sample and the electrode are immersed in cable oil to make the electrode contact closely with the sample and avoid the metal electrode edge Air discharge. The boosting method is rapid boosting, with a boosting rate of 500 V/s at a uniform rate. Five points of breakdown strength are taken for each test, and if the test specimen has a value deviation of more than 15%, Five more samples are to be taken.

The composite material breakdown data distribution meets the Weibull distribution, and the expression is:

$$F(E;\alpha,\beta) = 1 - \exp\left(-\left(\frac{E}{\alpha}\right)^{\beta}\right) \quad (1)$$

where: $F(t)$ is the probability of failure at a breakdown voltage less than or equal to t; E is the experimentally measured breakdown field strength (kV/mm); is the shape parameter of the breakdown voltage data, which characterizes the dispersion of the breakdown voltage data; α is the scale parameter of the test data representing the breakdown voltage at a failure probability of 63.2%, which characterizes the average breakdown voltage of the composite material.

3. Experimental Results

3.1. Conductive Current

The latter sample is abbreviated as EP-xSiC-ySiO_2, where x is the mass percentage of SiC filler and y is the mass percentage of SiO_2. Figure 2a shows the variation of conductivity with nanoparticle doping; the EP-ySiO_2 specimen has low conductivity and does not show non-linear conductivity characteristics; the composite conductivity increases with the increase in nanofiller content. Figure 2b shows the variation of the composite conductivity with micron SiC concentration for no nanoparticle doping. At a SiC doping of 20 wt%, the initial conductivity is low and shows a small increase at high fields. The micron SiC doping of 30 wt%–50 wt% shows similar ohmic conductivity characteristics at low electric fields. As the electric field intensity increases, the nonlinear conductivity electric field threshold decreases, and the nonlinear coefficient gradually increases with increasing micron SiC doping concentration. Figure 2c shows that at a nano SiO_2 doping concentration of 1 wt% and micron SiC doping concentration of 30 wt% or less, the ternary composite dielectric conductivity decreases compared to the micron composite, while the nonlinear slope increases compared to the EP-xSiC specimen.

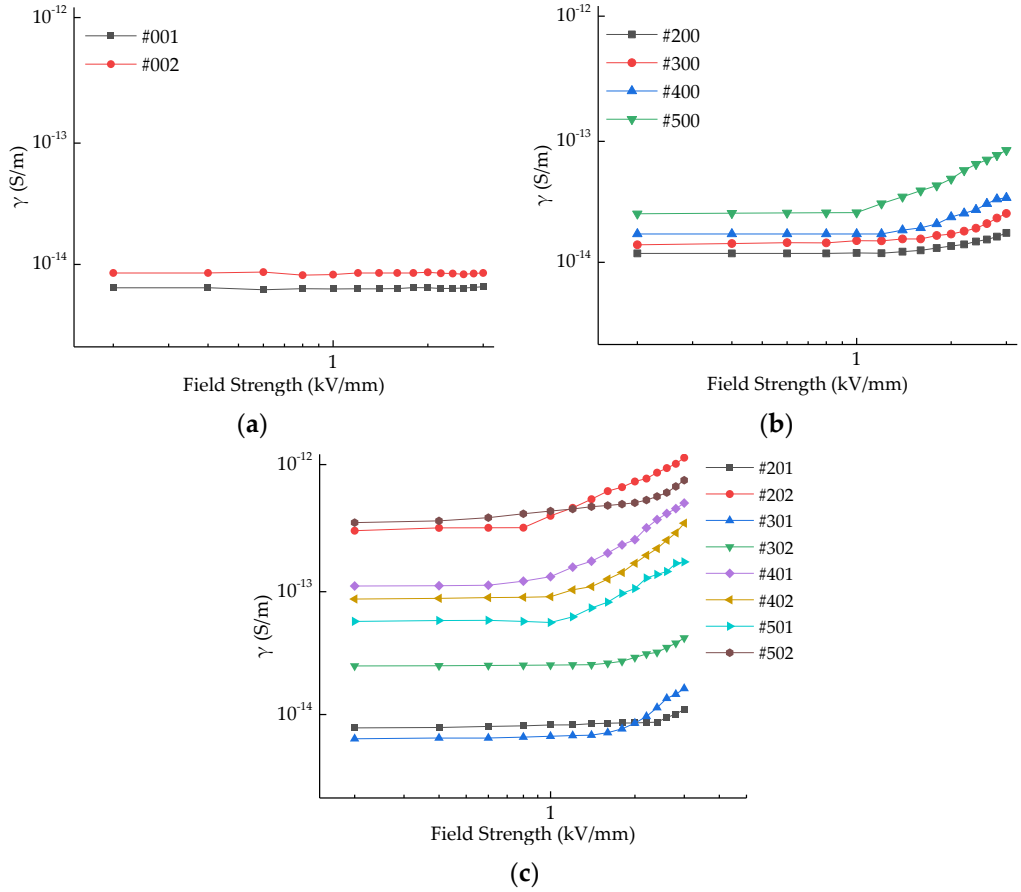

Figure 2. (**a**) The conductivity of nano SiO_2 doped specimen, (**b**) micron SiC/Epoxy composites, and (**c**) nano-micron hybrid composites.

The dielectric conductivity is determined by the carrier concentration and carrier mobility [14,15]. In the EP/SiC/SiO_2 ternary system, the impurity ions and electron conductivity are mainly used. Micro SiC filler, as a semiconductor crystal, has a narrow-forbidden bandwidth and a much higher probability of excitation of valence electrons than epoxy resin, while semiconductor doping usually introduces a large number of impurity ions, which increases the carrier concentration in the composite material and leads to an increase in conductivity. SiO_2 crystals also have a very wide forbidden band, and their conductivity is usually lower than 10^{-16} S/m. Therefore, the mechanism of the effect

of nano SiO_2 doping on conductivity can be excluded. The change in the conductivity of the composite after nano-doping can be explained by the nano-interface theory for the native conductivity of the particles. The selected nano SiO_2 has an average particle size of 80 nm and a specific surface area of 150 m^2/g, which has a large surface energy. When the nanoparticle surface is in contact with the epoxy resin matrix, the epoxy resin molecular chains in contact with the nano surface are restricted and show the result of the uniform arrangement, the atomic spacing decreases, and the two atomic potential fields interact so that the width and height of the original potential barriers decrease, and under the action of the applied electric field, the electron of the higher energy state will penetrate the potential barrier and transfer to another atom. Under the action of the applied electric field, the electrons in the higher energy state penetrate the barrier and transfer to the other atom. The regular arrangement of molecular chains due to the surface energy of nanoparticles may create a periodically changing potential field, but the arrangement of molecular chains may not reach the level of crystals, and their own forbidden bandwidth is much higher than that of semiconductors, so the irregular arrangement of individual nanoparticles cannot provide a crystal-like environment. When the concentration of nanoparticles increases, some of the nanoparticles have smaller spacing, the formed interfacial states overlap, and the interatomic degeneracy decreases significantly, the high-energy electrons can move freely in the periodic potential field formed in the interface, and the carrier concentration and conductivity in the local region increase at this time [14]. When the nano-doping concentration is low, the nano-dispersion is good, but the spacing is too far to form a conductive region that can affect the overall conductivity. When the nano-doping concentration is high, the agglomeration phenomenon occurs, and the nano-effect is lost [16], and the external crystalline region of micron level is presented, which provides bridging between epoxy resin molecules and intermolecular channels for carriers, and the conductivity increases. In summary, the effect of nano-doping is affected by the nano-dispersity on carrier migration, both promotion and inhibition, and its effect is determined by the nano-SiO_2 doping concentration and SiC doping concentration together. Therefore, it appears that the conductivity of the composite decreases when the SiC content of the EP-xSiC-1SiO_2 specimen is below 30 wt% and increases for the rest of the specimens.

3.2. Dielectric Strength

In this section, the effect of nano-doping concentration on the breakdown strength of composites in ternary composites is investigated, and micro-nanocomposites with micron concentration of 40 wt% are selected as breakdown specimens. The Weibull distribution of epoxy resin-based micro-and nanocomposites with different SiO_2 content specimens is shown in Figure 3. Weibull parameters of samples with different SiO_2 content are listed in Table 2.

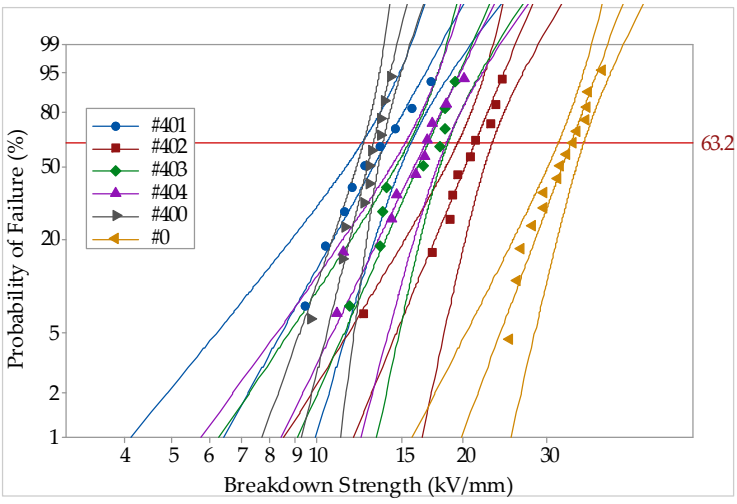

Figure 3. Weibull distribution of breakdown field strength of composites with different SiO_2 content.

Table 2. Weibull parameters of samples with different SiO_2 content.

Specimen	α (kV/mm)	β
#400	13.09	13.411
#401	13.39	4.611
#402	20.44	4.976
#403	17.02	7.391
#404	16.82	6.659

As shown in Figure 3, the breakdown voltage of the specimen with SiO_2 nano-doping is higher than that of the specimen with a single SiC doping, and the breakdown field strength of the composite medium increases with the increase in SiO_2 nano-doping content and reaches the highest at 2 wt% of the nano-doping concentration.

For a small amount of nano SiO_2 doping and the increase in the breakdown electric field of the composite material caused by the reason that the size of the nanofiller itself is less than 10 nm, and the forbidden bandwidth is extremely wide, its own conductivity is lower than that of the epoxy resin matrix, the atoms of the nanoparticles have a very high conductivity barrier, the nucleus of the atom is extremely strong binding capacity, the external performance of the deep trap, the carrier passes around the nanoparticles, low-energy electrons will be trapped. The breakdown strength increases as the carrier concentration decreases [17,18]. The reduction of the breakdown field of the composite material is related to the overlap of the nano-interface. The nano-fillers have a large specific surface area and the high surface energy can restrict the molecular chains on the surface of the nano-particles to form a regular arrangement in the local area and form a crystal-like structure [19], which will make the atoms in the molecular chains close to each other and the atomic potential field affect each other so that the width and height of the inter-atomic potential barriers are reduced and the original energy level is split. At this time, the forbidden band width of the epoxy resin matrix decreases, and under the action of the applied electric field, the high-energy electrons that accumulate energy in the crystal region can penetrate the potential barrier, which helps carriers migrate in the composite material while retaining enough energy, and finally leads to the reduction of breakdown field strength.

At the nano-SiO_2 doping concentration below 2 wt%, the nanoparticle spacing is large, the interface is isolated, the polymer potential barrier is large, the chance of electrons crossing the barrier remains small, and the interface thus traps low-energy electrons, resulting in a decrease in the total carrier mobility of the composite. As the nanofiller increases, the number of isolated interfacial structures increases and the carrier mobility decreases, which is reflected in the increase in breakdown field strength. When the nano-fillers continue to increase, the area where the interfacial region appears to be overlapped increases, the original energy levels of the energy bands become discrete, the original medium potential barrier decreases, electrons can migrate within a larger range of periodic potential fields, electrons can accumulate more energy, and the macroscopic expression is a decrease in breakdown field strength. Comparing the micro- and nano-doped specimens with the pure epoxy resin specimens, the maximum breakdown strength of the ternary specimens is still smaller than that of the epoxy, and at this micro- and nano-doping concentration, the hindering effect of nano-doping on carrier migration is smaller than the promoting effect of the micron filler on carrier migration.

4. Simulation Study on the Conductivity and Carrier Transport Mechanism of Micro and Nanocomposites

4.1. Micron SiC/EP Composite Model Finite Element Analysis

The micron SiC particles are irregularly granular in shape, and the SiC is set as a uniform size spherical model to reduce the computational effort, and the finite element models of the composites with four micron SiC doping concentrations are established. The

model parameters were set according to the concentration data of micron SiC used in the experimental preparation, and the model parameters are shown in Table 3.

Table 3. Geometric parameter setting of micron composite model.

Parameter Name	Numerical Value
Diameter of SiC	24 μm
Radius of EP model	400 μm
Thickness of EP model	100 μm
Density of SiC	3.2×10^3 (kg/m^3)
Density of EP	980 (kg/m^3)

According to the solid dielectric conductivity mechanism, the atomic distribution in the micron composite is irregular, and the crystal structure of SiC itself is not affected when dispersed into the organic non-crystalline medium and still retains its original properties [20]. The material properties are shown in Table 4. The material properties are shown in Table 4.

Table 4. Material property setting of micron composite model.

Micron SiC	Numerical Value	EP	Numerical Value
γ (S/m)	1×10^{-7}	γ (S/m)	1×10^{-15}
ε_r	3.97	ε_r	3.50

A micron dielectric model with SiC micron particle content of 10 wt%, 20 wt%, and 30 wt% were established, and we randomly generated micron particle spatial coordinates using the MATLAB random function rand, as shown in Figure 4, and the corresponding numbers of SiC micron particles are shown in Table 5. The first type of boundary conditions of the current physical field of the micron dielectric model is set as follows: the upper surface potential is 200 V, the lower surface grounded, constituting an applied electric field of 2 kV/mm.

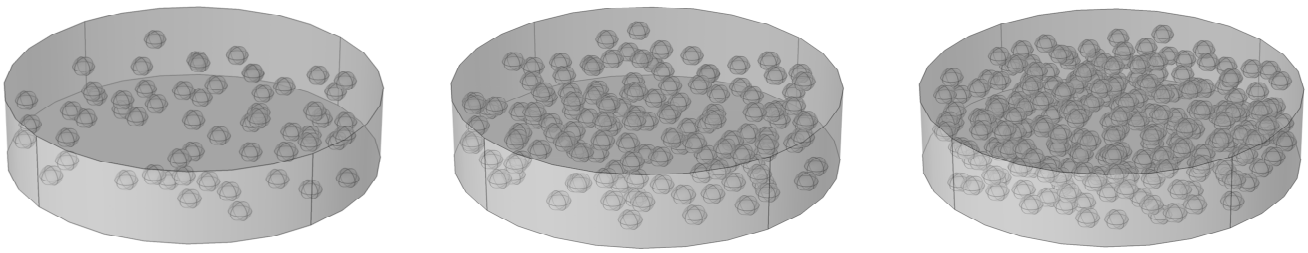

(**a**) (**b**) (**c**)

Figure 4. Different SiC doped EP/SiC composite models. (**a**) 10 wt% SiC; (**b**) 20 wt% SiC; (**c**) 30 wt% SiC.

Table 5. The number and spacing of SiC particles in the micro dielectric model with the different filling amounts.

Doping Concentration of SiC	10 wt%	20 wt%	30 wt%
Spacing of micron particles/μm	50	32	23
Number of SiC micron particles	59	133	226

4.1.1. Potential Distribution under a Constant Electric Field

Taking the micron SiC doping content of 20 wt% as an example, the potential distribution cloud at an applied electric field of 2 kV/mm is shown in Figure 5a, and the potential varies uniformly over the epoxy resin according to the law shown in the potential cloud distribution. The volume current density under this electric field is shown in Figure 5b, and its bulk average current density is calculated as 6.71×10^{-9} A/m^2, compared with

the current density of #200 specimen in Figure 2a as 2.74 × 10^{-8} A/m^2, which is similar in order of magnitude and proves that the simulation results are reliable.

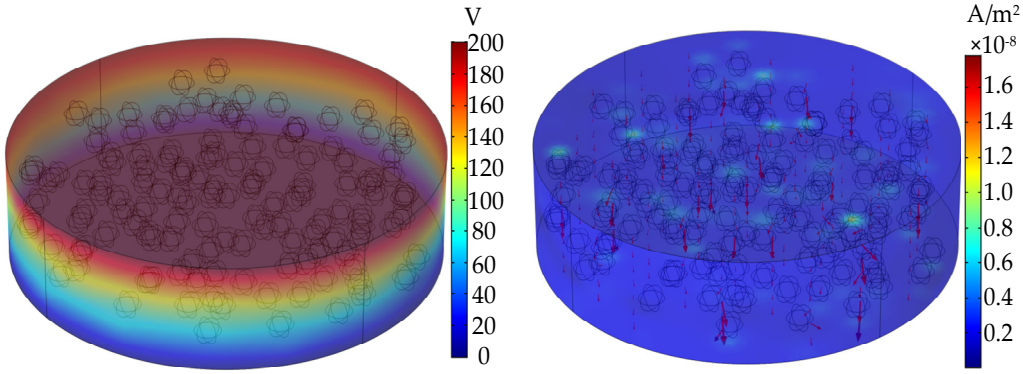

(**a**) (**b**)

Figure 5. Potential and current density distribution diagram. (**a**) Potential distribution; (**b**) current density distribution.

4.1.2. Electric Field Distribution of SiC Cut Surface

The electric field simulation clouds of the composite model with micron doping concentration of 10 wt%, 20 wt%, and 30 wt% under 2 kV/mm electric field are shown in Figure 6, from which it can be seen that the dielectric electric field of the composite material is more uniform in the matrix or SiC, which is approximately equal to the applied electric field, and the dielectric tunneling effect is not obvious under this electric field, and the dielectric conductance at this time is mainly caused by the electrons on the SiC conduction band under the action of thermal vibration The dielectric conductance at this time is mainly formed by the electrons in the SiC conduction band crossing the potential barrier under the effect of thermal vibration and forming a jump conductance between the crystalline region, but there is a strong electric field concentration at the interface between SiC and epoxy resin matrix, and the maximum value of cross-sectional electric field increases from 2 kV/mm to 9.5 kV/mm, 13.4 kV/mm and 19.1 kV/mm, which indicates that the electric field at the interface of SiC is much higher than the applied electric field even when the applied electric field is low, and the magnitude of the interfacial electric field increases with the concentration of micron SiC, and this concentration phenomenon decreases the potential barrier at the interface and promotes the tunneling effect at the same time.

The variation of the electric field at the interface of the composites by applying voltages of 2 kV/mm–4 kV/mm to the models with micron doping of 10 wt%, 20 wt%, and 30 wt%, and taking the maximum electric field intensity within the model, the simulation results are shown in Table 6.

Table 6. Maximum interface electric field intensity under different external electric fields.

Applied Electric Field (kV/mm)	Maximum Electric Field at Interface (kV/mm)		
	10 wt%	20 wt%	30 wt%
2	16.16	19.43	20.17
2.2	17.78	21.37	22.19
2.4	19.40	23.31	24.20
2.6	21.01	25.26	26.22
2.8	22.63	27.20	28.24
3	24.25	29.14	30.26
3.2	25.86	31.09	32.27
3.4	27.48	33.03	34.29
3.6	29.10	34.97	36.31
3.8	30.71	36.91	38.32
4	32.33	38.86	40.34

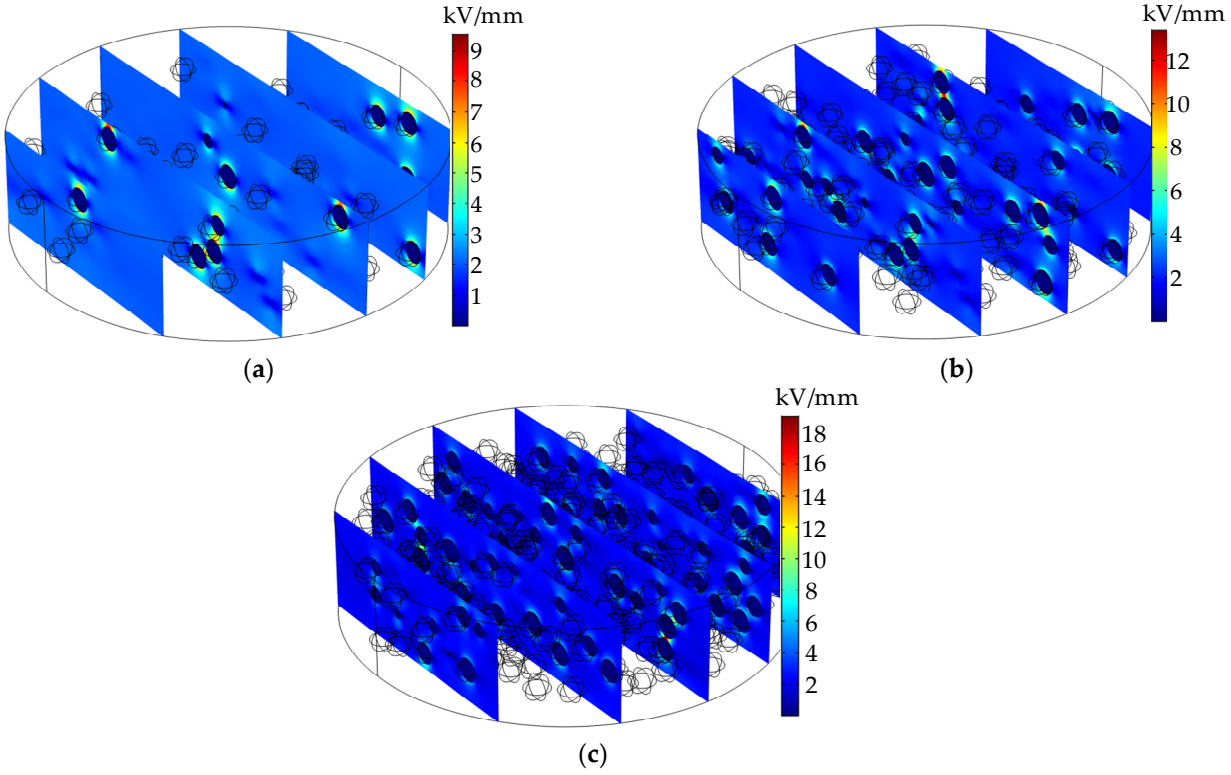

Figure 6. Cross-section of the electric field of the compound model under a constant electric field. (**a**) 10 wt% SiC; (**b**) 20 wt% SiC; (**c**) 30 wt% SiC.

Analyzing the data in Table 6, the intensity of the interfacial electric field increases by about 8 times, 9.5 times, and 10 times compared with the macroscopic electric field under the three SiC doping concentrations, respectively. This phenomenon indicates that the higher the micron SiC doping content has a greater effect on the internal electric field, while the change of the interfacial electric field decreases when it increases to a certain concentration, which is because the increase in the content leads to the decrease in the particle spacing, so that the interparticle potential changes rapidly, resulting in the electric field intensity increases.

Analyzing the data in Table 6, the interfacial electric field strength increases about 8 times, 9.5 times, and 10 times, respectively, compared with the macroscopic electric field under the three SiC doping concentrations; this phenomenon indicates that the higher the micron SiC doping content, the greater the influence on the internal electric field, while increasing to a certain concentration, the interfacial electric field change decreases, this is because the increase in content leads to the reduction of particle spacing, so that the interparticle potential changes rapidly, resulting in the electric field This phenomenon of local electric field rise leads to the decrease in overall breakdown field of the composite.

4.2. Nanocomposite Model

When the trap filling effect is not considered, the possibility of electron delocalization is small, so the simulation model only simulates the process of carrier capture into the trap. The multi-shell layer model of SiO_2 nanoparticles is constructed according to Tanaka's description of the nano-interface, and the spherical interface is divided into three layers: the first layer is the bonding layer, which corresponds to the inorganic-to-organic transition layer tightly bound by coupling agents; the second layer is the binding layer, which corresponds to the polymer chains strongly bound or interacting with the first layer and the inorganic particle surface The third layer is the loose layer, which is a loosely coupled region that interacts with the second layer [21]. According to the multishell layer mechanism of nanodielectric made by Tanaka, the thickness of the interface formed by nanoparticles is

between 10 nm and 30 nm, and the thickness of the first bonding layer should be between 2 nm and 9 nm, so the three interface thicknesses are set as 5 nm, 10 nm, and 15 nm, as shown in Figure 7. Due to the strong surface interaction energy of nanoparticles, which restricts the motion of molecular chain segments around the particles, the three layers show an elevated relative permittivity at the macroscopic level, so the relative permittivity of the bonded layer is assumed to be 2, the bound layer is 3, and the loose layer is 3.5.

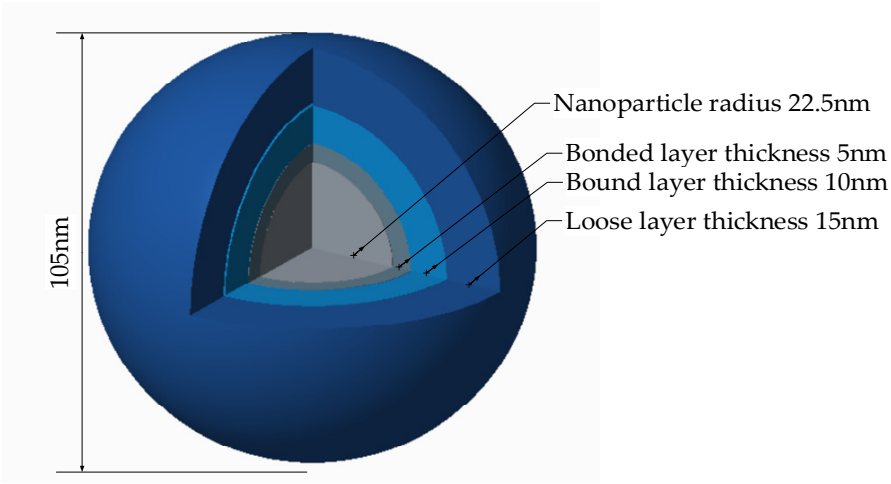

Figure 7. Multi-shell model of SiO_2 nanoparticles.

To study the effect of nano-interfaces on carrier migration, randomly distributed multishell SiO_2 nanoparticles were added to the epoxy resin as charge traps to simulate the process of carrier capture by charge traps. Jiasheng et al. derived the energy levels and densities of deep and shallow traps in the epoxy resin-based SiO_2 nano dielectric based on the Simmons theory of surface potential decay, according to which the energy levels and densities of deep and shallow traps were set [22,23] The trap depths of deep and shallow traps are 0.99 eV and 0.925 eV, and the densities of deep and shallow traps are 2.8×10^{18} and 2.2×10^{18} $eV^{-1} \cdot m^{-3}$. The bonding layer is set to a deep trap and 1.11 eV above the trap depth of the substrate itself, and the loose layer is set to a shallow trap of 0.93 eV, stopping the motion of the particles when the electrons pass through the trap range if the energy is below the trap depth. The trap will capture the carriers injected into the substrate material, and the capture chance is usually determined according to the capture cross-section, which is larger for the shallow trap than the deep trap, so the shallow and deep trap cross sections are set to 10^{-14} m^2 and 10^{-16} m^2 [24]. As there is a certain law for the distribution of nanoparticles in the medium, the distance between two adjacent nanoparticles at a certain concentration in the ideal case of no agglomeration is [25]:

$$d = r\left\{\left[\frac{4\pi}{3}\left(1+\frac{1-F}{F}\frac{\rho_F}{\rho_m}\right)\right]^{\frac{1}{3}} - 2\right\} \quad (2)$$

where r is the nanoparticle radius; F is the mass fraction of nanoparticles; ρ_F and ρ_m are the densities of nanoparticles and polymer matrices, respectively. According to the trap cross-section and trap density and nanoparticle content, the spatial coordinates of nanoparticles are randomly generated using MATLAB random function rand to build a SiO_2/epoxy nano-dielectric model with SiO_2 nanoparticle content of 1%, 2%, and 3%, respectively, as shown in Figure 8, and the corresponding number of SiO_2 nanoparticles is shown in Table 7. Set the electrostatic field boundary conditions of the nano-dielectric model: the lower surface potential is 3.5 V, the upper surface is grounded, and the electron emission inlet is set to the upper surface. Table 7 Number and spacing of SiO_2 nanoparticles in the nano dielectric model with different filling amounts.

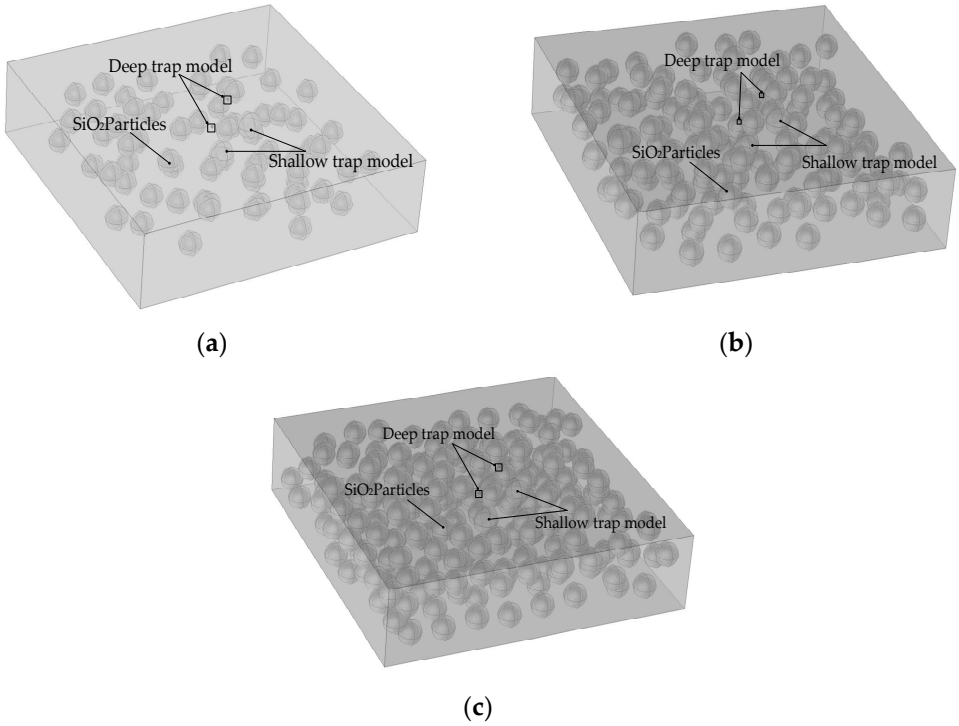

Figure 8. Nano-doping concentration is (**a**) 1 wt%, (**b**) 2 wt%, (**c**) 3 wt% epoxy resin/SiO_2 composite model.

Table 7. The number and spacing of SiO_2 nanoparticles in the nano-dielectric models with different filling amounts.

	1 wt%	**2 wt%**	**3 wt%**
Nanoparticle spacing/nm	221	176	153
Number of SiO_2 nanoparticles	66	135	204

4.3. Analysis of Electron Motion State and Spatial Charge

The Schottky emission current, as the input current of the material, was used, and the number of input electrons was fixed at 1000 electrons to observe the motion trajectory of electrons after entering the epoxy resin matrix. Figure 9 shows the motion of electrons at each doping concentration. Assuming that the obstruction effect of the epoxy resin matrix on the electron motion is ignored, when the electrons enter the medium, only a small part is trapped, and the rest all enter the inside of the medium. Based on the epoxy resin matrix model, when 1 wt%, 2 wt%, and 3 wt% of SiO_2 nanoparticles are added inside the epoxy resin, part of the electron motion is restricted by the internal potential barrier and cannot enter the medium (the arrow in the figure represents the location of the charge and the direction of electron motion). The presence of nanoparticles provides a large number of deep and shallow traps, resulting in charge trapping near the cathode, and the hindering effect on the injected charge becomes stronger with the increase in nanoparticle doping concentration.

Figure 10 shows the space charge distribution on the surface of the composite anode for different nano-doping contents. Due to the small size of the model compared to the size of the anti-corona layer of the motor wire rod, which can be considered as only one point, the charge concentration in the conforming model is not discussed. In pure epoxy resin, the surface space charge is 3.1×10^{-4} C/m^2, and the surface space charge density of nanocomposite anodes at 1 wt%, 2 wt%, and 3 wt% nano-doping concentrations all show regions of lower surface space charge density at local locations and the regions of lower space charge density increase as the nano-doping concentration increases. The average

surface space charge on the anode surface of each specimen was averaged, as shown in Table 8, and the average surface charge density gradually decreased with the increase in nano-doping concentration, reflecting that nano-doping has a good inhibitory effect on space charge aggregation.

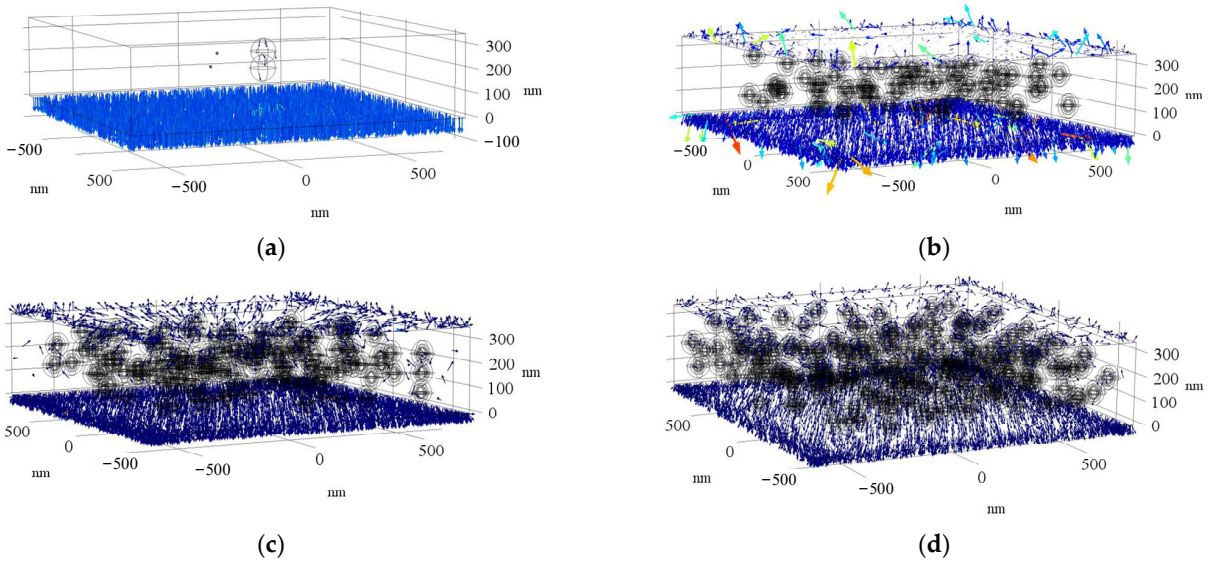

Figure 9. Electron motion state with nano doping concentration of (**a**) 0 wt%, (**b**) 1 wt%, (**c**) 2 wt%, (**d**) 3 wt%.

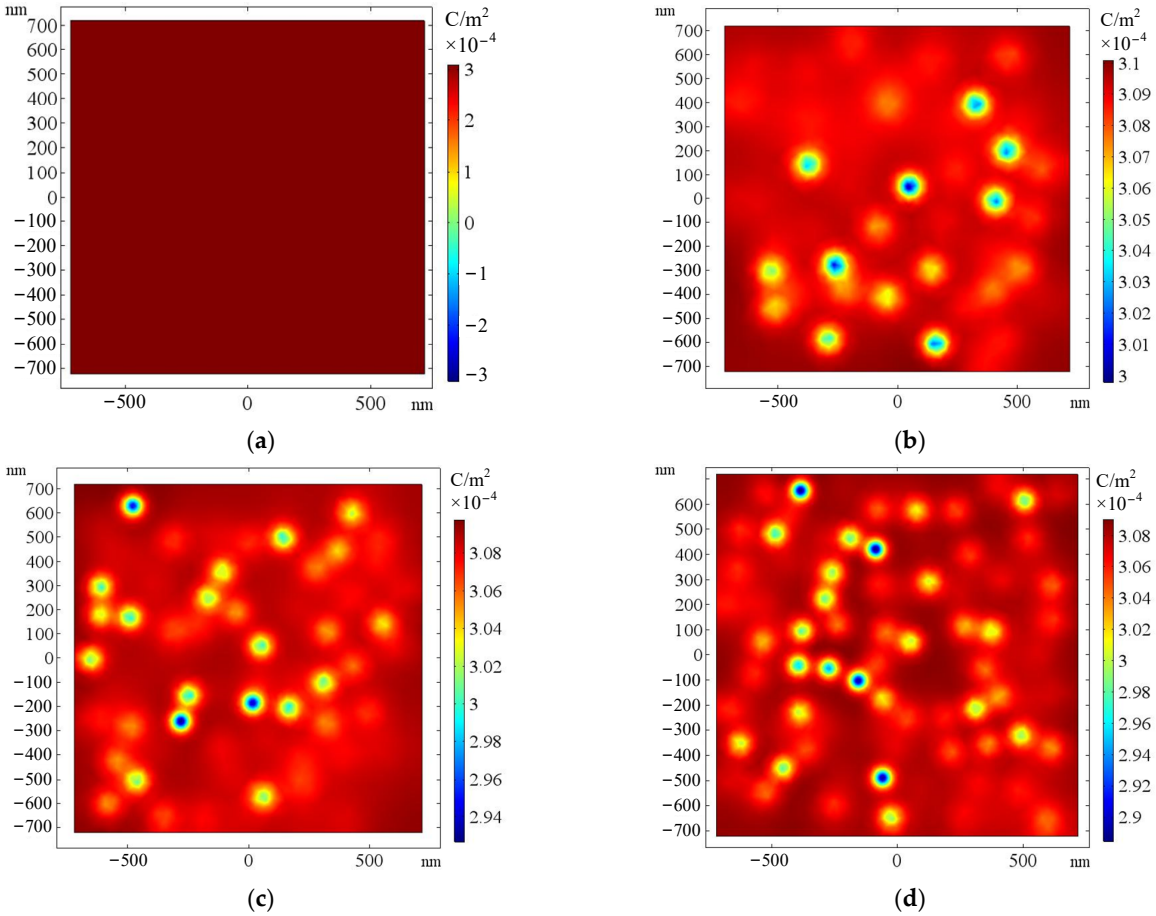

Figure 10. The nanoSiO_2-doping concentration is (**a**) 0 wt%, (**b**) 1 wt%, (**c**) 2 wt%, (**d**) 3 wt% anode surface charge density.

Table 8. The average surface space charge density of pure epoxy resin and SiO_2/epoxy resin nano-dielectric.

Dielectric	Average Surface Charge Density/(C/m^2)
EP	3.10×10^{-4}
1 wt%	3.09×10^{-4}
2 wt%	3.08×10^{-4}
3 wt%	3.07×10^{-4}

5. Conclusions

The effects of filler doping concentration on the DC conductivity characteristics and AC breakdown characteristics of the composites were investigated by preparing a ternary composite system of epoxy resin, micron SiC, and nano SiO_2; the finite element model was constructed in COMSOL to analyze the effects of micro and nano doping on the electric field distribution and the electron transport process inside the composites, and the following conclusions were drawn.

1. The conductivity characteristics of micro-nanocomposites are related to the dispersion of inorganic particles, and the dispersion of nano-SiO_2 is also affected by the doping concentration of micron SiC. When the doping concentration of SiC is 20 wt%, the dispersion of nano-particles is better at low concentrations, and the nano-effect shows deep traps. When SiO_2 is aggregated, the linked SiO_2 will form uniformly arranged crystalline regions, increasing the range of electron-free movement, reducing the jump potential barrier between crystalline regions, and showing the trend of increasing conductivity.
2. The breakdown field strength of the composites decreases with the increase in SiC content when the doping content of nano-SiO_2 is the same, and the breakdown field strength of the composites tends to increase and then decrease with the increase in nano-SiO_2 concentration when the micron SiC content is the same. When the concentration of nano-SiO_2 is small, it will show the tendency to obstruct the carrier movement and reduce the electron-free travel, thus increasing the breakdown voltage of the composites.
3. The calculated results of the electric field model at the EP/SiC interface show that inside the dielectric doped with micron SiC, the electric field near the particle surface appears to be concentrated, and the electric field intensity at the interface increases exponentially relative to the applied electric field intensity, and the maximum electric field intensity at the interface increases to 40 kV/mm at 30 wt% doping.
4. The increase in nanofiller concentration can make the electrode injected charge in the shallow layer of the medium gather, weaken the internal electric field there, more effectively inhibit the subsequent electrode charge injection into the medium, reduce the medium space charge and increase the medium breakdown field strength in the case of good dispersion of nanoparticles.

Author Contributions: Conceptualization, N.G.; Investigation and Formal analysis, R.M.; Project administration, J.G.; Resources, M.H.; Funding acquisition and Supervision, Y.Z.; Validation, L.H.; Methodology, H.H.; Software, R.M. and H.H.; Writing—original draft, R.M.; Writing—review & editing, N.G., J.G. and H.H. All authors have read and agreed to the published version of the manuscript.

Funding: This research was funded by Project of National Science Foundation of China, 51577045; and Postdoctoral Research Startup Fund Project of Heilongjiang Province of China, LBH-Q19106. And The APC was funded by Project of National Science Foundation of China, 51577045.

Institutional Review Board Statement: Not applicable.

Informed Consent Statement: Not applicable.

Conflicts of Interest: The authors declare no conflict of interest.

References

1. Frigione, M.; Lettieri, M. Recent Advances and Trends of Nanofilled/Nanostructured Epoxies. *Materials* **2020**, *13*, 3415. [CrossRef] [PubMed]
2. Yuan, P.; Wang, H. Design and Simulation Analysis of Anti-Corona Structure at the End of the Stator Bar of Large Hydrogenerators. In Proceedings of the 2021 IEEE International Conference on Electronic Technology, Communication and Information, ICETCI, Changchun, China, 27–29 August 2021; pp. 77–83.
3. Han, Y.S.; Li, S.T.; Min, D.M. Space Charge Distribution and Nonlinear Conduction of Epoxy Nanocomposites. *Sens. Mater.* **2017**, *29*, 1159–1168. [CrossRef]
4. Jiang, H.; Zhang, X.; Gao, J.; Guo, N. Dielectric and AC Breakdown Properties of SiO_2/MMT/LDPE Micro–Nano Composites. *Energies* **2021**, *14*, 1235. [CrossRef]
5. Oh, D.-H.; Kim, H.-S.; Shim, J.-H.; Jeon, Y.-H.; Kang, D.-W.; Lee, B.-W. Characteristics of Gel Time and Dielectric Strength of Epoxy Composite According to the Mixing Ratio of Micro-Fillers. *Energies* **2020**, *13*, 5165. [CrossRef]
6. Naveen, J.; Babu, M.S.; Sarathi, R.; Velmurugan, R.; Danikas, M.G.; Karlis, A. Investigation on Electrical and Thermal Performance of Glass Fiber Reinforced Epoxy–MgO Nanocomposites. *Energies* **2021**, *14*, 8005. [CrossRef]
7. Wang, S.; Yu, S.; Li, J.; Li, S. Effects of Functionalized Nano-TiO_2 on the Molecular Motion in Epoxy Resin-Based Nanocomposites. *Materials* **2020**, *13*, 163. [CrossRef]
8. Maji, P.; Choudhary, R.; Majhi, M. Structural, optical and dielectric properties of ZrO_2 reinforced polymeric nanocomposite films of polymethylmethacrylate (PMMA). *Optik* **2016**, *127*, 4848–4853. [CrossRef]
9. Wang, X.; Chen, Q.; Yang, H.; Zhou, K.; Ning, X. Electrical properties of epoxy/ZnO nano-composite. *J. Mater. Sci. Mater. Electron.* **2018**, *29*, 12765–12770. [CrossRef]
10. Darani, S.Z.; Naghdabadi, R. An experimental study on multiwalled carbon nanotube nanocomposite piezoresistivity considering the filler agglomeration effects. *Polym. Compos.* **2021**, *42*, 4707–4716. [CrossRef]
11. Shukla, M.K.; Sharma, K. Effect of Carbon Nanofillers on the Mechanical and Interfacial Properties of Epoxy Based Nanocomposites: A Review. *Polym. Sci.-Ser. A* **2019**, *61*, 439–460. [CrossRef]
12. Kausar, A. Nanocarbon and macrocarbonaceous filler–reinforced epoxy/polyamide: A review. *J. Thermoplast. Compos. Mater.* **2020**. [CrossRef]
13. Muthukumaravel, C.; Karunakaran, U.; Mangamma, G. Local grain-to-grain conductivity in an SnO_2–V_2O_5 nanocomposite ethanol sensor. *Nanotechnology* **2020**, *31*, 344001. [CrossRef] [PubMed]
14. Haghgoo, M.; Ansari, R.; Hassanzadeh-Aghdam, M. Predicting effective electrical resistivity and conductivity of carbon nanotube/carbon black-filled polymer matrix hybrid nanocomposites. *J. Phys. Chem. Solids* **2021**, *161*, 110444. [CrossRef]
15. Fiolhais, M.C.N. The Cabibbo-Kobayashi-Maskawa density matrices. *Eur. Lett.* **2012**, *98*, 51001. [CrossRef]
16. Liu, S.; Chevali, V.; Xu, Z.; Hui, D.; Wang, H. A review of extending performance of epoxy resins using carbon nanomaterials. *Compos. Part B Eng.* **2018**, *136*, 197–214. [CrossRef]
17. Dagar, J.; Yadav, V.; Tyagi, P.; Singh, R.K.; Suman, C.K.; Srivastava, R. Effect of reduction of trap charge carrier density in organic field effect transistors by surface treatment of dielectric layer. *J. Appl. Phys.* **2013**, *114*, 224504. [CrossRef]
18. Jeong, I.-B.; Kim, J.-S.; Lee, J.-Y.; Hong, J.-W.; Shin, J.-Y. Electrical Insulation Properties of Nanocomposites with SiO_2 and MgO Filler. *Trans. Electr. Electron. Mater.* **2010**, *11*, 261–265. [CrossRef]
19. Owolabi, T.O.; Saleh, T.A.; Olusayo, O.; Souiyah, M.; Oyeneyin, O.E. Modeling the Specific Surface Area of Doped Spinel Ferrite Nanomaterials Using Hybrid Intelligent Computational Method. *J. Nanomater.* **2021**, *2021*, 9677423. [CrossRef]
20. Chi, Q.G.; Cui, S.; Zhang, T.D.; Yang, M.; Chen, Q.G. SiC/SiO_2 filler reinforced EP composite with excellent nonlinear conductivity and high breakdown strength. *IEEE Trans. Dielectr. Electr. Insul.* **2020**, *27*, 535–541. [CrossRef]
21. Tanaka, T. Multi-Core Model for Nanodielectrics as Fine Structures of Interaction Zones. In Proceedings of the Annual Report-Conference on Electrical Insulation and Dielectric Phenomena, Nashville, TN, USA, 16–19 October 2005; Volume 2005, pp. 713–716.
22. Ru, J.; Min, D.; Ma, B.; Pan, S.; Xing, Z.; Li, S. Influence of Surface Trap Parameters on DC Flashover in Vacuum of Epoxy Composites. In Proceedings of the CMD 2016-International Conference on Condition Monitoring and Diagnosis, Xi'an, China, 25–28 September 2016; pp. 1008–1011.
23. Simmons, J.G.; Tam, M.C. Theory of Isothermal Currents and the Direct Determination of Trap Parameters in Semiconductors and Insulators Containing Arbitrary Trap Distributions. *Phys. Rev. B* **1973**, *7*, 3706–3713. [CrossRef]
24. Williams, C.K. Kinetics of Trapping, Detrapping and Trap Generation. *J. Electron. Mater.* **1992**, *21*, 711–720. [CrossRef]
25. Duan-Lei, Y.; Dao-Min, M.; Yin, H.; Dong-Ri, X.; Hai-Yan, W.; Fang, Y.; Zhi-Hao, Z.; Xiang, F.; Sheng-Tao, L. Influence of filler content on trap and space charge properties of epoxy resin nanocomposites. *Acta Phys. Sin.* **2017**, *66*, 097701. [CrossRef]